RSC Advances

This article can be cited before page numbers have been issued, to do this please use: Q. Gong, S. Gong, H. Zhang, L. Liu and Y. Wang, *RSC Adv.*, 2015, DOI: 10.1039/C5RA08521G.

ROYAL SOCIETY OF CHEMISTRY

www.rsc.org/advances

View Article Online
DOI: 10.1039/C5RA08521G

Synthesis of a novel polyimide used as liquid crystal vertical alignment layers

Qing Gong[a], Shiming Gong[a], Heng Zhang[a], Lulu Liu[a], Yinghan Wang[a]*

[a] *State Key Laboratory of Polymer Materials Engineering, College of Polymer Science and Engineering, Sichuan University, Chengdu 610065, China. Email: wang_yh@scu.edu.cn; Tel: +86-28-8546-0823; Fax: +86-28-8546-0823*

A novel functional diamine containing triphenylamine moiety and biphenyl, N,N-bis(4- aminophenyl)-4-(biphenyl)-4'-aminophenyl ether (N0), was successfully synthesized and characterized. A series of polyimides (PIs) and poly(amic acid)s (PAAs) had been synthesized from cyclobutane-1,2,3,4-tetracarboxylic dianhydride (CBDA), 2,2'-bis(trifluoromethyl)-[1,1'-biphenyl]-4,4'-diamine (TFDB), 4-dodecyloxy-phenyl-4',4''-diaminotriphenylamine (C12) and the newly synthesised diamine monomer (N0) through a conventional two-step procedure that included a ring-opening polyaddition to give polyamic acids, followed by thermal cyclodehydration. Pretilt angles of liquid crystal (LC) cell fabricated with the PIs were measured, and rubbing resistance of PIs containing different side chain structure was investigated. PI1 with rigid biphenyl side chain could induce LC parallel alignment after rubbing process. Although PI3 containing flexible alkyl side chain could induce LC vertical alignment before rubbing process, it only induced LC parallel alignment after rubbing process. However, PI2 containing both rigid biphenyl side chain and flexible alkyl side chain could induce LC vertical alignment before and after rubbing process. A new method for improving rubbing resistance of PIs and a generation mechanism of rubbing resistance had been proposed. In addition, all PI films showed high thermal stability and high transmittance in the wavelength range of 400-700 nm.

1. Introduction

Aromatic polyimides (PIs), which have outstanding thermal, mechanical, and

View Article Online
DOI: 10.1039/C5RA08521G

chemical stability, attracted a lot of scientific and commercial interest [1]. These polymers have been widely used in many fields such as membrane materials for separation,[2,3] composites,[4-6] high temperature coatings[7] as well as alignment layers in liquid crystal displays (LCDs).[8,9]

When it comes to LCDs, there is so much wish for its good performance such as a wide viewing angle, a high contrast ratio and a fast response time. However, the conventional LCD like STN-LCD performance has been unsatisfactory due to a narrow viewing angle and a slow response time. Thus, several approaches for improving the viewing angle have been brought up, such as the addition of birefringence films,[10] the domain divided twisted nematic,[11] the in-plane-switching (IPS) mode[12,13] and the multi domain vertical alignment (MVA) mode.[14-18]. The MVA-LCD could be very promising to achieve a wide viewing angle, fast response time, and high contrast ratio at the same time. In this kind of display,[14] a homeotropic PI layer has been used as the liquid crystals (LCs) alignment layer, which aligns LCs vertically at the field-off state and the pretilt angle has to be controlled above 88^{o} after a rubbing process. It is usually accepted that the generation of the pretilt angles is highly dependent upon the interactions of the PIs with LCs.[19] Some reports further pointed out that the high pretilt angle could be achieved using the PIs with bulky side chains composed of rigid units and long alkyl chains as the alignment layer.[20] Xia Senlin and his coworkers synthesized a series of PIs containing a 6-hexyloxy-naphthalen side chain, which had good aligning ability and the pretilt angles were above 89^{o}.[8] Liu Zhijie and her coworkers prepared a series of PIs with (*n*-alkyloxyl)biphenyl group, which could align LCs vertically when *n* was more than 6.[21] However, previous works mainly focused on the solubility of PIs and high pretilt angles without serious consideration of the equally important thing rubbing resistance. It is well known that rubbing process is currently the only technique applied in the LCD industry to treat PI film surfaces in the mass-production of flat-panel LCD devices. The rubbing treatment could enhance uniformity of LCs alignment and give an excellent performance to LCDs. Therefore, PI used as LCs vertical alignment layers must have a good rubbing resistance, so that PI films could still induce LCs

View Article Online
DOI: 10.1039/C5RA08521G

vertical alignment after rubbing process. Obviously, the approach to enhance the rubbing resistance is worth paying enough attention to.

The objective of this work was to synthesize a novel polyimide used as liquid crystal vertical alignment layers and put forward a new method by introducing rigid biphenyl chains into PIs to improve the rubbing resistance of PIs. Consideration to high pretilt angle and good rubbing resistance, we focused on a specially designed PI obtained from copolycondensation among N,N-bis(4-aminophenyl)-4-(biphenyl)-4'-aminophenyl ether (N0) containing rigid biphenyl moiety, 4-dodecyloxy-phenyl-4',4''-diaminotriphenylamine (C12) containing flexible alkyl moiety, 2,2'-bis(trifluoromethyl)-[1,1'-biphenyl]-4,4'-diamine (TFDB) and cyclobutane-1,2,3,4-tetracarboxylic dianhydride (CBDA) as the alignment layer. Properties such as optical transparency, thermal stability, and pretilt angle were investigated. In addition, the mechanism of rubbing resistance was preliminarily explained by a diagram of side chain structure in PIs. The new method for improving rubbing resistance of PI films will hopefully be applied in vertical-alignment-mode LCD devices.

2. Experiment section

2.1 Materials

4-fluoronitrobenzene, biphenyl-4-ol, 1-chloro-4-nitrobenzene, potassium carbonate (K_2CO_3), hydrazine hydrate and cesium fluoride (CsF) were purchased from Aladdin Chemical Reagent Corp. (shanghai, China). Dimethyl sulfoxide (DMSO) and N-methyl-2-pyrrolodone (NMP) were obtained from Bodi Chemical Reagents Corp. (Tianjin, China), and then distilled at a reduced pressure after stirring over calcium hydride for 24 h and stored over 4 Å molecular sieves before use. CBDA (>98%) was attained from Zhongtiansheng Technology co., Ltd., and purified by recrystallisation from acetic anhydride and then dried in vacuum prior to use. TFDB was gained from Shanghai EMST Corp. (Shanghai, China) and used after recrystallisation from ethanol. Nematic LC E7 (n_o=1.521, Δn = 0.22, T_{N-L} = 60°C) was obtained from Yantai

View Article Online
DOI: 10.1039/C5RA08521G

Xianhua Chem-Tech Co., Ltd. (Yantai, China). All the other solvents and chemicals were used as received and without further purification, unless otherwise specified.

2.2 Measurements

Nuclear magnetic resonance (^{1}H-NMR) spectra was measured on a 400 MHz Unity INVOA 400 spectrophotometer with DMSO-d_6 or $CDCl_3$-d as the solvent and tetramethylsilane (TMS) as the internal reference. Fourier transform infrared spectra (FT-IR) was recorded on a Nicolet 560 FT-IR spectrophotometer. Thermogravimetric analysis (TGA) was taken from a DuPont TGA 2100 at a heating rate of 10 ^{o}C/min under a nitrogen atmosphere. The rubbing process was operated with a rubbing machine from TianLi Co. Ltd. (Chengdu, China). Spin-coating process was executed using a KW-4A spinner from institute of microelectronics of Chinese Academy of Science (Beijing, China).The pretilt angles of LC cells were measured by crystal rotation method using a pretilt angle tester from Changchun Institute of Optics, Fine Mechanics and Physics (Changchun, China), and at least five different points on cells were selected for measurement. The surface morphology of the PI films before and after rubbing was investigated by atomic force microscopy (AFM) operating in tapping mode using an instrument with a SPI4000 Probe Station controller (SIINT Instruments Co., Japan) at room temperature. Olympus tapping mode cantilevers with spring constants ranging from 51.2 N/m to 87.8 N/m (as specified by the manufacturer) were used with a scan rate in the range of 0.8–1.2 Hz. Polarising microscope from Shanghai Millimeter Precision Instrument Co. Ltd. (Shanghai, China) was used to evaluate the alignment behaviours of LCs. Contact angles of a deionized water and methylene iodide on the surface of the polyimide films were measured by a Kruss DSA100 goniometer system (Kruss GmbH, Germany). A Young's harmonic-mean equation was applied to predict the surface tensions from the contact angles. Gel permeation chromatography (GPC) of soluble polymers was performed using an Applied Bio system (Foster City, CA, USA) at 70 ^{o}C with two PL gel 5μm mixed-C columns (Agilent, Santa Clara, CA, USA).

View Article Online
DOI: 10.1039/C5RA08521G

2.3 Synthesis of monomer

2.3.1 Synthesis of 4-(p-nitrophenoxy)biphenyl (a). A mixture of 150 mL of DMF, 7.25 g (46.0 mmol) of 1-chloro-4-nitrobenzene, 7.53 g (44.3 mmol) of biphenyl-4-ol and 11.06 g (80.0 mmol) of K_2CO_3 was placed into a 250-mL round-bottomed flask equipped with a magnetic stirrer and a condenser. The mixture was stirred and heated to 150 ^oC. After 8 h, the reaction was stopped and the mixture was allowed to cool to room temperature. Then the mixture was poured into 300 mL of distilled water to yield pale-yellow precipitates. The precipitate was collected by filtration and repeatedly washed with distilled water. Finally, the product was recrystallized with dichloromethane to gain 11.35 g (yield: 88 %) of crystals.

^{1}H-NMR (DMSO-d_6), δ (ppm): 7.29, 8.28 (m, 4H, ArH–NO_2), 7.70, 7.20, 7.79, 7.49, 7.39 (m, 9H, Ar–H of biphenyl). FT-IR (KBr, pellet), cm^{-1}: 1568, 1506, 1484 (aromatics), 1247, 1168 (C–O–C).

2.3.2 Synthesis of 4-(p-aminophenoxy)biphenyl (b). A mixture of 10.14 g (34.8 mmol) of 4-(p-nitrophenoxy)biphenyl (a), 1.02 g of 5 % palladium on activated carbon (Pd/C) and 80 mL of ethanol was placed into a 250-mL round-bottomed flask equipped with a magnetic stirrer and a condenser. The mixture was stirred and heated to reflux, and then 80 % hydrazine hydrate (8.70 g, 174.0 mmol) was added dropwise into the mixed solution. The mixture was refluxed for 4 h and filtered subsequently to remove Pd/C. Then the solvent was evaporated, and the crude product was finally recrystallized with ethanol to gain 8.46 g (yield: 93 %) of solid.

^{1}H-NMR (DMSO-d_6), δ (ppm): 5.03 (s, 2H, NH_2), 6.61, 6.81 (m, 4H, ArH–O–), 6.93, 7.31, 7.43, 7.60 (m, 9H, Ar–H of biphenyl). FT-IR (KBr, pellet), cm^{-1}: 3398, 3326, 3221 (NH_2), 1503, 1484 (aromatics), 1224, 1199 (C–O–C).

2.3.3 Synthesis of N,N-bis(4-nitrophenyl)-4-(biphenyl)-4'-aminophenyl ether (c). A mixture of the aromatic ether-amine 4-(p-aminophenoxy)biphenyl (b) (7.49 g, 28.6 mmol), p-fluoronitrobenzene (8.47 g, 60.0 mol), CsF (12.96 g, 85.8 mmol), and DMSO (60 mL) was placed into a 250-mL three-necked flask equipped with a magnetic stirrer, a nitrogen inlet, and a condenser. The mixture was stirred and heated

View Article Online
DOI: 10.1039/C5RA08521G

to 150 ^{o}C. After 8 h, the reaction mixture was cooled and poured into 70 mL of methanol. The yellow precipitate was collected by filtration. The product was washed with water and dried. Finally, the crude product was purified by recrystallisation from methanol to afford 10.53 g (yield: 79 %) yellow crystals.

^{1}H-NMR (DMSO-d_6), δ (ppm): 8.20, 7.22 (m, 8H, ArH-NO_2), 7.31, 7.18 (m, 4 H, –O–ArH), 7.74, 7.66, 7.47, 7.46, 7.25 (m, 8 H, Ar-H of biphenyl). FT-IR (KBr, pellet), cm^{-1}: 1500, 1485 (aromatics), 1580, 1340 (NO_2), 1241, 1112 (C–O–C).

2.3.4 Synthesis of N,N-bis(4- aminophenyl)-4-(biphenyl)-4'-aminophenyl ether (N0). A mixture of 9.67 g (19.2 mmol) of N,N-bis(4-nitrophenyl)-4-(biphenyl)-4'-aminophenyl ether (c), 0.97 g of 5 % Pd/C and 55 mL of ethanol was placed into a 100-mL round-bottomed flask equipped with a magnetic stirrer and a condenser. The mixture was stirred and heated to reflux, and then 80 % hydrazine hydrate (9.62 g, 192.0 mmol) was added dropwise into the mixed solution. The mixture was refluxed for 4 h and filtered subsequently to remove Pd/C. Then the solvent was evaporated. The crude product was finally recrystallized with ethanol to gain 7.58 g of crystals (yield: 89 %).

^{1}H-NMR (DMSO-d_6), δ (ppm): 4.96 (s, 4H, NH2), 6.54, 6.82 (m, 8H, NH_2–ArH), 6.66, 6.86 (m, 4H, −O–ArH), 6.99, 7.32, 7.44, 7.61 (m, 9H, Ar–H of biphenyl). FT-IR (KBr, pellet), cm^{-1}: 3456, 3335 (NH_2), 1623, 1495 (aromatics), 1228, 1110 (C–O–C).

2.4 Synthesis of the polymer

The PIs and PAAs were synthesized from commercial dianhydride CBDA, the auxilliary diamine TFDB and two functional diamines (N0 or C12). The molar ratios of N0, C12 and TFDB were controlled to be 2:0:8 (PI1 or PAA1), 1:1:8 (PI2 or PAA2) and 0:2:8 (PI3 or PAA3) to obtain the PIs and the PAAs.

The synthesis of PI2 and PAA2 was used as an example to illustrate the general synthetic route used to prepare the PIs and PAAs. The typical procedure was as follows: 0.07 mmol of N0, 0.07 mmol of C12 and 0.56 mmol of TFDB were dissolved in 2.05g of NMP in a 50-mL three-necked flask with a stirrer. After a clear solution was formed, 0.7 mmol of CBDA was added to the solution. And the final

View Article Online
DOI: 10.1039/C5RA08521G

mixture was stirred at room temperature under a gentle flow of dry nitrogen for 24 h to yield viscous PAA2 solutions. The PAA2 was converted into polyimide via a thermal imidization process. For the thermal imidization method, the PAA2 solution was cast onto a clean glass plate and heated (80 ^{o}C for 30 min, 120 ^{o}C for 30 min, 200 ^{o}C for 1 h, 240 ^{o}C for 2 h) to produce a fully imidized PI2 film.

2.5 Fabrication of the LC cells

The PAA solutions were diluted to a solid content of 5 wt% in NMP. The solutions attained were coated onto clean glass substrates by spin-coating at a rotation speed of 600 rpm for 15 s, then 2500 rpm for 30 s, followed by heating at 80 ^{o}C for 30 min to evaporate the solvent. Then the films were heated at 250 ^{o}C for 1 h to complete thermal imidization. The cured PI films on glass were rubbed with a roller covered with rayon velvet fabric, and the rubbing strength (RS) was calculated as follows (*RS*=28.5 mm in this work):

$$RS = NM\left(\frac{2\pi rn}{60v}\text{-}1\right)$$

where *RS* (mm) was the total length of rubbing cloth that touched a certain point of the films; *N* was the cumulative number of rubbings (N=1 in this work); *M* (0.3 mm) was the contact length of the rubbing roller circumference; v (17.2 mm/s) was the velocity of the substrate stage; *n* (700 rpm) and *r* (22.5 mm) were the rubbing roller speed and radius, respectively.

The LC cells were made from two pieces of the rubbed PI films in an antiparallel rubbing direction with 45-μm-thick PI film spacers. Besides, some non-rubbed substrates were also used to fabricate LC cells for comparison. The LC cells gap were filled with a nematic LC E7 using a capillary method at 80 ^{o}C, and then the injection hole was sealed with photosensitive epoxy glue. The LC cells were then heat-treated for 20 min at 80 ^{o}C, which was higher than the nematic-to-isotropic transition temperature of E7, to eliminate flow marks. The alignment behaviors of the LC cells were examined with polarized optical microscopy. The pretilt angles of the LCs were measured using a crystal rotation method.

View Article Online
DOI: 10.1039/C5RA08521G

3. Results and discussion

3.1 Monomer synthesis

The diamine 4-dodecyloxy-phenyl-4',4''-diaminotriphenylamine (C12) used as one of the functional diamine was synthesized according to our previously work.[22] Four steps were employed in synthesizing the novel functional diamine N0 from biphenyl-4-ol, as shown in Scheme1.

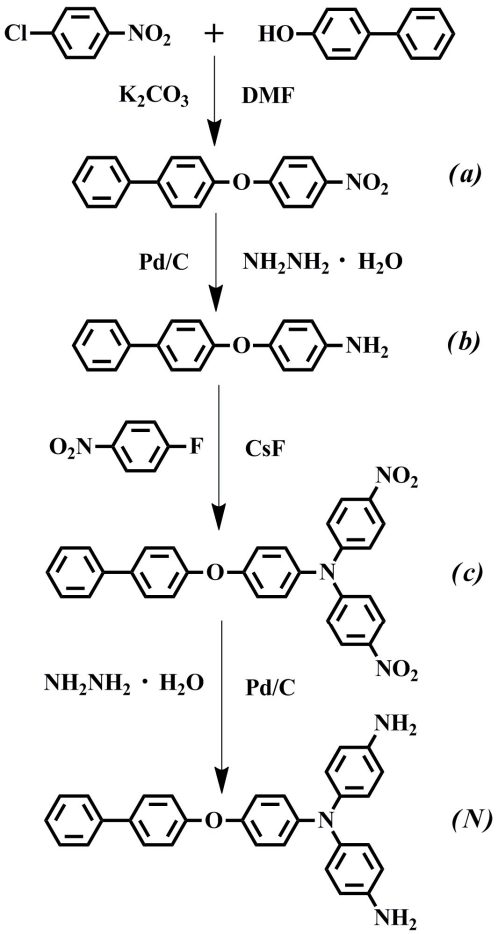

Scheme 1 Synthetic route to the functional diamine N0

First, 4-(p-nitrophenoxy)biphenyl (a) was prepared via an aromatic nucleophilic substitution (S_NAr) reaction of 1-chloro-4-nitrobenzene with biphenyl-4-ol in DMF in the presence of K_2CO_3 as an acid acceptor. Subsequently, **a** was reduced to 4-(p-aminophenoxy)biphenyl (b) by means of Pd/C and hydrazine hydrate. The target diamine monomer N,N-bis(4-aminophenyl)-4-(biphenyl)-4'-aminophenyl ether (N0)

View Article Online
DOI: 10.1039/C5RA08521G

was synthesized by double N-arylation reactions of **b** with two equivalents of p-fluoronitrobenzene in the presence of CsF, followed by hydrazine hydrate Pd/C-catalyzed reduction of the intermediate dinitro compound N,N-bis(4-nitrophenyl)-4-(biphenyl)-4'-aminophenyl ether (**c**).

The chemical structures of all of the above compounds were confirmed by their FT-IR and ^{1}H-NMR spectra. All of the spectroscopic data obtained were consistent with the proposed structures. A typical ^{1}H-NMR spectrum of compound **N0** was illustrated in Fig.1.

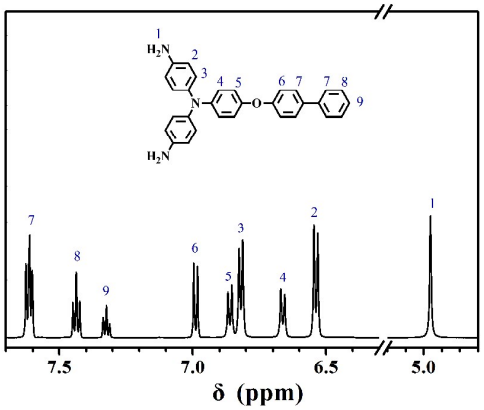

Fig. 1 The ^{1}H-NMR (400 MHz) spectrum of the functional diamine N0 in DMSO-d_6

3.2 Polymer synthesis

New PIs were prepared from N0, C12, TFDB, and CBDA via a conventional two-step procedure, as shown in Scheme 2. The polymerization was carried out by reacting stoichiometric amounts of the diamines with aromatic dianhydrides at a concentration of 15 % solids in NMP. Ring-opening polymerization at room temperature for 24 h yielded the PAA solution, followed by a thermal imidization, subsequent gradually heating from room temperature to 240 ^{o}C to obtain the corresponding PIs.

View Article Online
DOI: 10.1039/C5RA08521G

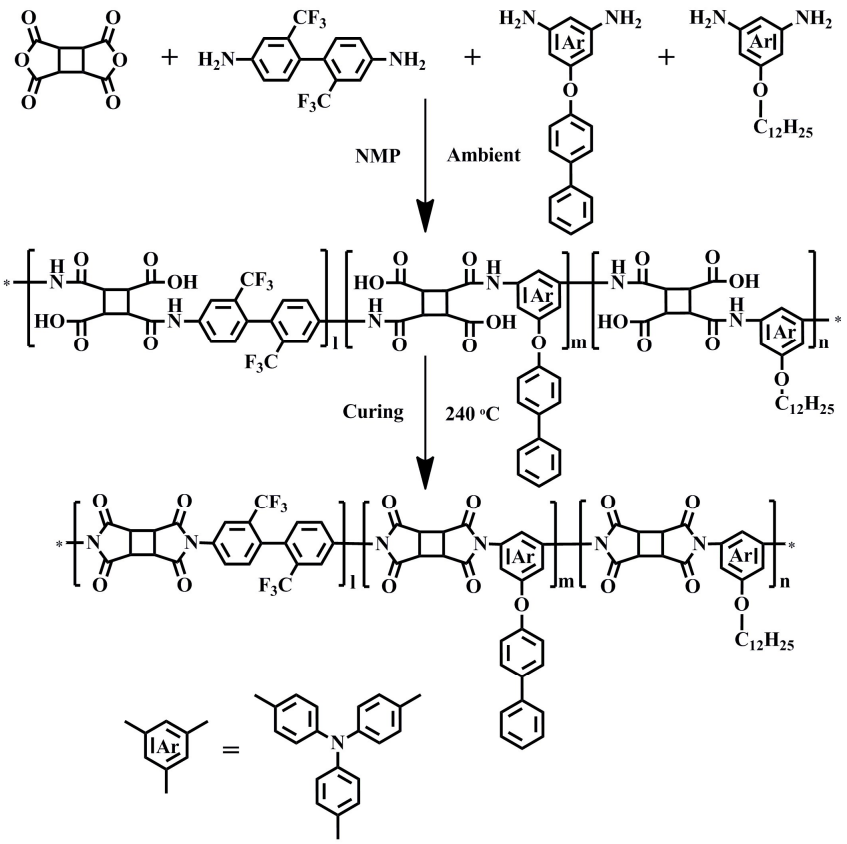

Scheme 2 Synthetic route to the polymers

The formation of the PAAs and PIs was confirmed with ^{1}H-NMR and FT-IR. As an example, the ^{1}H-NMR spectrum of PAA2 was shown in Fig.2. The broad peak at 10.1–10.3 ppm was the characteristic peak of the amide protons, the peak at 10.6-10.9 ppm was the characteristic peak of the carboxyl protons and the peaks at 6.8–8.4 ppm were the characteristic peaks of the phenyl ring protons of the PAA. The FT-IR spectrum of PIs presented in Fig. 3 showed typical absorption bands of aliphatic C–H stretching at 2928–2851 cm^{-1} corresponding to the methyl groups of the diamine C12. The peak intensity of PI2 was weaker than PI3's since the content of the diamine C12 of PI2 was half of PI3. Absorptions at 1781 cm^{-1} and 1724 cm^{-1} were observed due to the asymmetric and symmetric C=O stretching vibrations of the imide groups, respectively. Absorption at 1370 cm^{-1} was assigned to C–N stretching, absorptions at 1174–1135 cm^{-1} to C–F stretching, and a sharp absorption band at around 748 cm^{-1} to the skeletal vibrations of the imide rings. There were no characteristic absorption

View Article Online
DOI: 10.1039/C5RA08521G

bands of the amide group near 3200–3363 cm^{-1} (N–H stretching) and 1650–1674 cm^{-1} (C=O stretching), indicating that the polymers had been fully imidized.[23,24]

In addition, the GPCs of all PAAs were investigated, and the data was listed in Table 1, which indicated high molecular weights in the range 1.41-1.64×10^4 g/mol for M_n. The molecular weights were quit up to requirement of the liquid crystal alignment layers.

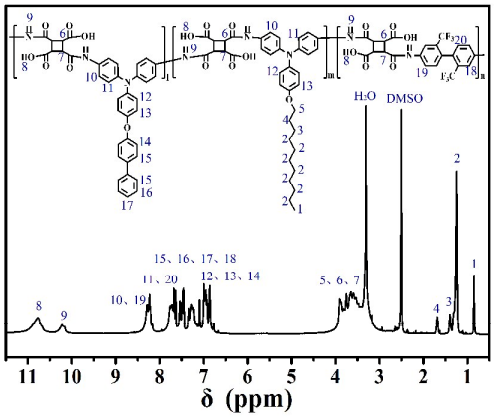

Fig. 2 ^{1}H-NMR (400 MHz) spectrum of PAA2 in DMSO-d_6

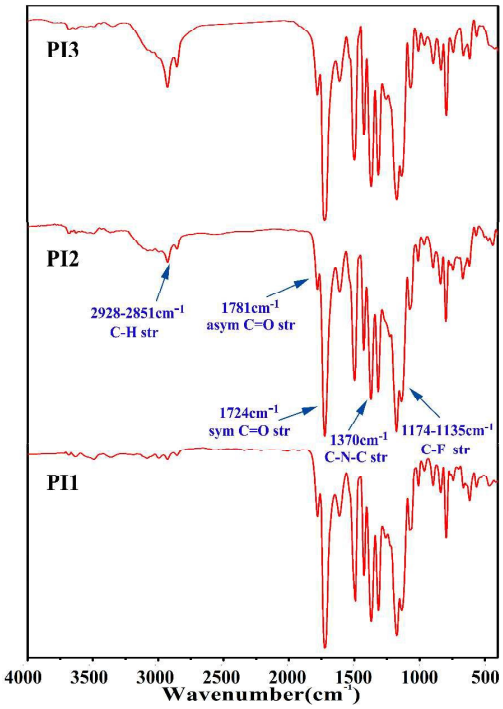

Fig. 3 Thin film FT-IR spectrum of PIs

View Article Online
DOI: 10.1039/C5RA08521G

Table 1 Formula and GPC molecular weights of PAAs

PAAs	N0:C12:TFDB:CBDAa	Mn (10^{-4} g/mol)b	Mw/Mn
PAA0	20:0:80:100	1.41	1.93
PAA2	10:10:80:100	1.44	1.97
PAA3	0:20:80:100	1.64	2.05

[a] Composition of monomers were calculated as mole ratio.

[b] Number-average molecular weight calculated by GPC in THF versus polystyrene standards.

3.3 Optical transparency

The transmittances of PIs were investigated using a UV–vis spectrophotometer at room temperature. All PI films were obtained by casting from a 5 wt% PAA solution on a calcium fluoride (CaF_2) piece at room temperature, and subsequent sequential heating to 240 ^{o}C for 2 h, then PI films were gained by immersion the glass plate in water followed by drying in an oven at 100 ^{o}C. The thickness of all PIs was around 10 μm. The UV–vis spectra of the PI films was shown in Fig.4. All of the PI films showed high transmissions in the wavelength range 400–700 nm, which was attributed to existence of aliphatic dianhydride (CBDA) that blocked charge transformation in the molecular chains, fluorine atoms of TFDB that was good for optical transparency, and large side units that increased the distance and blocked charge transformation between molecular chains. The similar optical transmittance of PIs was attributed to the same content of the function diamines (N0 and C12). The high optical transparency of the PI films was advantageous in LCD devices.

View Article Online
DOI: 10.1039/C5RA08521G

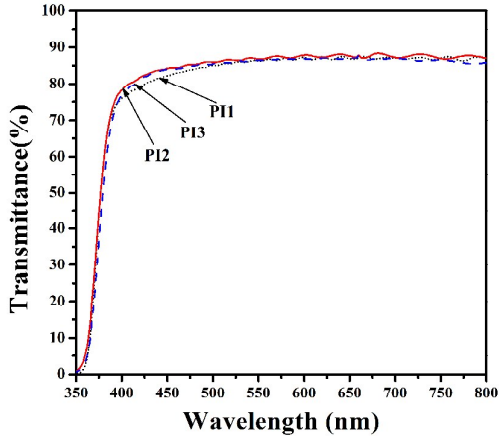

Fig. 4 UV–vis transmission spectra of PI films (film thickness: 10 μm)

3.4 Thermal properties

Thermal stabilities of the PIs films were studied by TGA under a nitrogen atmosphere and their programs were reproduced in Fig.5. The initial thermal decomposition temperature (T_d), temperature at which a weight loss of 5% occurred (T_5), temperature at which a weight loss of 10% occurred (T_{10}), and the residual weight at 800 ^{o}C (R_w) were summarized for all PIs in Table 1. As Fig.5 showed, two-stage thermal decomposition behavior was observed, which was similar to the behavior of those other reported polymers.[25,26] The first step at relatively lower temperatures, presumably, was ascribable to degradation of the side chains. As the results of Differential Thermal Gravity (DTG) show, the speed on loss in weight of PIs increased with the increasing content of the long alkyl side chains. Compared with PI1, PI2 and PI3 contained the same number of functional diamine (N0 or C12), the PI1 exhibited the best thermal stabilities since its side chains contained more benzene rings and fewer alkyl units. The second step at relatively higher temperatures probably resulted from the thermal degradation of the rigid aromatic backbones. The introduction of bulky, twisted triphenylamine (TPA) group into PIs increased the rigidity of the backbone of PIs, thus, all PIs exhibited a higher values of T_{10}. The TGA results showed that all PIs performed good thermal stability.

View Article Online
DOI: 10.1039/C5RA08521G

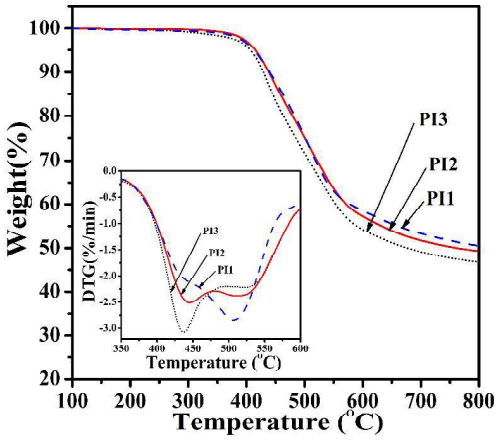

Fig. 5 TGA thermograms of PIs, obtained at a scan rate of 10 °C/min (inset: Differential Thermal Gravity (DTG) of PIs).

Table 2 The thermal properties of the PIs

PIs[a]	T_d[b] (°C)	T_5[b] (°C)	T_{10}[b] (°C)	R_w[b] (°C)
PI1	373	420	444	50.0
PI2	360	422	440	49.3
PI3	328	410	435	46.8

[a] Measured samples were obtained by the chemical imidization method.

[b] T_d was the decomposition onset temperature; T_5 and T_{10} were the temperatures at which weight losses of 5% and 10% occur; R_w was the residual weight (%) at 800 °C in nitrogen.

3.5 Alignment properties of LCs

3.5.1 pretilt angles. The pretilt angle, which greatly determines the electro-optical properties of LCD devices, is affected by a lot of factors, such as the surface morphology, steric effects and the electronic interaction of the LC with the alignment layer. All of these factors are related to the processing conditions used, such as the rubbing treatment, as well as the chemical structure of the PI. As is well known, rubbing treatment is a technique that is widely used to obtain homogeneous alignment of the LC molecules on the polymer surface. This paper concentrated on the effect of rubbing on the pretilt angles of the LC cells.

View Article Online
DOI: 10.1039/C5RA08521G

All pretilt angles before and after rubbing process were measured by a crystal rotation method and their numerical values were listed in Table 2. As shown in the table, the LCs was not aligned on the surface of the PI1 film without the rubbing treatment. On the other hand, the pretilt angles of the LC cell fabricated with PI2 and PI3 with long flexible alkyl side chain were 90° before the rubbing process. These results indicated that long flexible alkyl side chain was necessary for vertical alignment of LCs. After rubbing process, the pretilt angle of LCs on PI1, PI2 and PI3 film were 4.5°, 89.7° and 2.4°, respectively. That is to say, PI2 containing both rigid biphenyl side chain and flexible alkyl side chain could still induce LC vertical alignment after rubbing process, but PI1 only containing rigid biphenyl side chain and PI3 only containing flexible alkyl side chain induced LC parallel alignment.

Table 3 Pretilt angles of the LC cells fabricated with the PIs

PIs	Pretilt angle θ_p (°)	
	Before rubbing	After rubbing
PI1	No alignment	4.5
PI2	90	89.7
PI3	90	2.4

3.5.2 Alignment behavior. A high pretilt angle is crucial to obtain good optical and electrical performances for vertical alignment LCDs. Besides, the uniformity of LCs vertical alignment at a large area is also important. Consequently, it is necessary to investigate the uniformity of LCs alignment on the PI films. The uniformity of LCs alignment was examined between crossed polarisers with a polarising optical microscope. As shown in Fig. 6 **a** and **c**, after rubbing process, an alternate and periodical change of transmittance with the rotation of the substrate stage could be observed, meaning that the LC molecules in cells using PI1 and PI3 were aligned planar to the PI surface. Fig. 6 **b** showed that the transmittance of the LC cells using the rubbed PI2 with a rotation of the sample stage gave no rise to an alternate and periodic appearance of darkness and brightness, meaning that the LC molecules were

View Article Online
DOI: 10.1039/C5RA08521G

aligned vertical to the PI surface. Conoscope observation of the cells was used with polarized optical microscope. In Fig.6 **b**, the dark crossed brush was clearly seen and did not move with the LC cell rotating under conoscope. The result further proved that PI2 containing both rigid biphenyl side chain and flexible alkyl side chain could introduce the LCs vertical alignment, and it also suggested that PI2 film was more resistance to rubbing process.

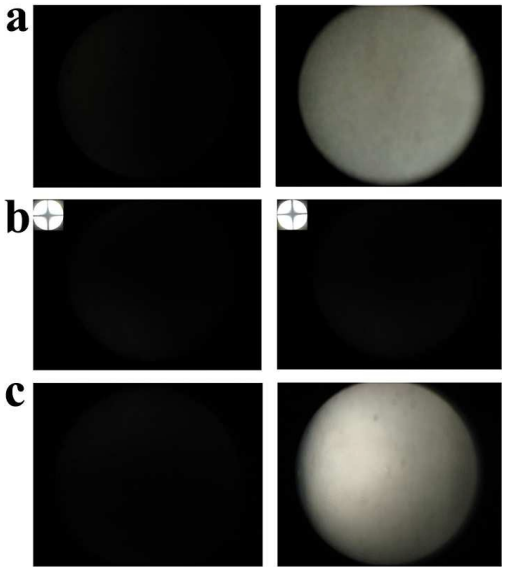

Fig. 6 Polarized optical microscopic images of LC cells using the rubbed PI1 (a), PI2 (b) and PI3(c). All pictures were captured under crossed polarizers. The conoscopic images are shown in the corners of the images. The micrographs on the right hand side were taken for cells after rotating the stage by 45°.

3.5.3 Surface energy. The surface energy could supply some information about the surface of PI films for researching the alignment behavior of the LCs. As shown in Fig. 7, the surface energy of the PI films was measured before and after the rubbing treatment. Compared with PI1, the surface energy of PI2 and PI3 was significantly decreased with the introduction of flexible alkyl side chains, which resulted in a high pretilt angle 90^{o}. That is, the surface polarity of the PI films was decreased with the introduction of the nonpolar alkyl side chains. After rubbing treatment, the surface energy of PI1 and PI2 were slightly increased, and the surface energy of PI3 had a

View Article Online
DOI: 10.1039/C5RA08521G

more marked increase compared to PI1 and PI2. That is, for PI3, the rubbing process induced the increase of the polarity of the polyimide films by an insertion of the nonpolar alkyl side chains into the polymer bulk phase during the rubbing process, which resulted in change of a geometric structure of the polyimide thin films and the increase of a flatness of thin film to make the liquid crystal molecules to lie flater.[27] For PI2, the insertion of the nonpolar alkyl side chains into the polymer bulk phase during the rubbing process was difficult to appear because of the existence of the rigid biphenyl side chains, which could restrict the movement of the alkyl chains. So, the results of surface energy also suggested that PI2 film was more resistance to rubbing process.

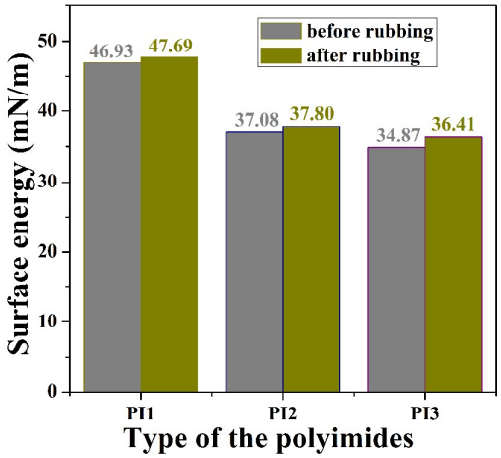

Fig. 7 Surface energy of the PIs before and after the rubbing process.

3.5.4 Surface morphology. Surface morphology of PI1, PI2 and PI3 films was measured by AFM before and after rubbing process. Parts A, B and C of Fig. 7 were shown the AFM images of PI1, PI2 and PI3 films before rubbing treatment, respectively. It was found that the PI1, PI2 and PI3 films had a root-mean-square (RMS) roughness of 0.31, 0.46 and 0.34 nm over an area of 2.5×2.5 μm^2. The surface morphology and roughness of the PI film derived mainly from the characteristics of the polymer chains that govern the aggregation and molecular ordering that occurred during the drying and thermal imidization processes after spin-casting.[28] In contrast, after rubbing treatment, as show in Fig. 7 D, E and F, all PIs films exhibited microgrooves along the rubbing direction. The formation of

View Article Online
DOI: 10.1039/C5RA08521G

microgroove lines might be attributed to the shear-induced deformation of the polymer films surface induced by the contact of fibers during the rubbing process. The developed microgrooves of the rubbed PI1, PI2 and PI3 films were around 38 nm or larger in size. The RMS surface roughness values of the rubbed PI1, PI2 and PI3 films were 1.31, 1.29 and 1.36 nm over an area of $2.5 \times 2.5 \ \mu m^2$, respectively.

From the above alignment results of LCs and surface morphology results of PIs films, although the PI1, PI2 and PI3 films had same morphologies after rubbing treatment, only PI2 could induce LC molecules vertical alignment, and PI1 and PI3 induced LCs parallel alignment. Besides, the microgrooves developed along the rubbing direction were much larger in size than the LC molecules. These facts suggested that the LC molecules were more likely to be aligned by interactions with the polymer chain segments, rather than by the microgrooves. Further, some reports had pointed out that there were some intermolecular interactions between LC molecules and the side chains of PIs, such as the dipole-dipole and π-π interaction between the biphenyl groups of LC molecules and the biphenyl groups of side chains, as well as the van der Waals forces between the alkoxy end-group of PI and the flexible alkoxy tail in an LC molecules. Due to the strong mutual interactions, LC molecules tended to be aligned in the direction parallel to the biphenyl groups of the side chains in the PI films.[25, 29]

Therefore, it was believed that the molecular chain reorientation, especially the side chain, had a greater influence on the LCs aligning ability on the PI film surfaces than the microgrooves did. After rubbing process, PI2 containing both rigid biphenyl side chain and flexible alkyl side chain could still induce LCs vertical alignment, but PI3 only containing flexible alkyl side chain induced LCs parallel alignment. The reason was that, in PI3, the flexible alkyl side chain might easily be reoriented toward the polymer bulk phase by the rubbing process. However, in PI2, the rigid biphenyl side chain might restrict the movement of the alkyl chain into the polymer surface, which resulted in an enrichment of alkyl side chain at the outmost layer of the PI surface.

View Article Online
DOI: 10.1039/C5RA08521G

Consequently, based on the result of pretilt angles, surface energy and surface morphology, a generation mechanism of rubbing resistance could be proposed, which was shown in Scheme 3. As shown, the alkyl side chain of the PI2 containing the rigid biphenyl side chain might be more difficultly reoriented toward polymer bulk phase than that of the PI3 with flexible alkyl side only.

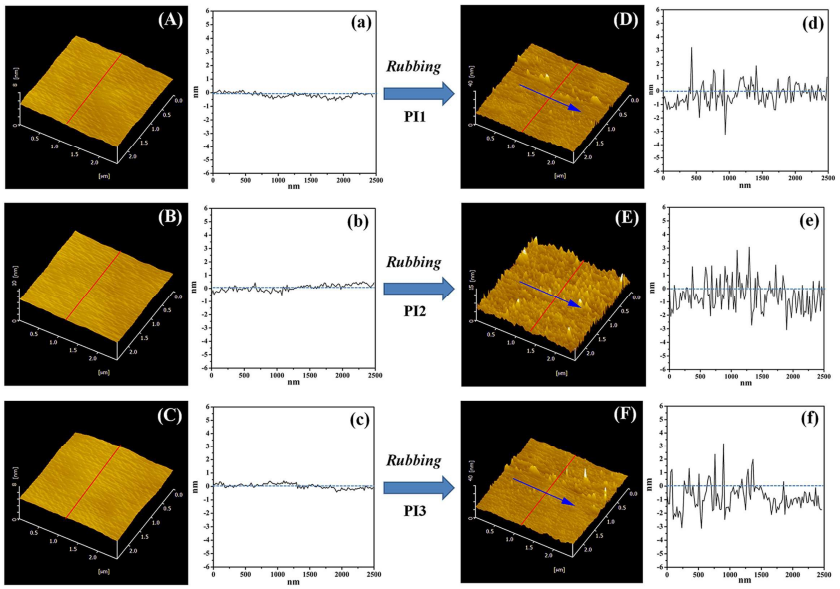

Fig. 8 AFM images and surface profiles of PI films before and after rubbing: (A) and (a) pristine PI1; (B) and (b) pristine PI2; (C) and (c) pristine PI3; (D) and (d) rubbed PI1; (E) and (e) rubbed PI2; (F) and (f) rubbed PI3. The arrows in the images (D), (E) and (F) denote the rubbing direction, respectively.

View Article Online
DOI: 10.1039/C5RA08521G

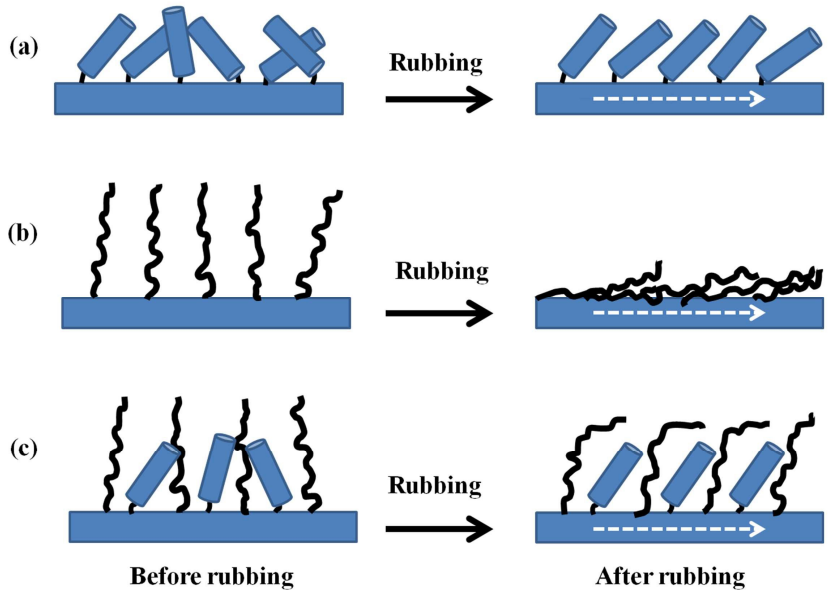

Scheme 3 Proposed mechanism of the microscopic molecular reorientation of the PIs surface induced by the rubbing process (a) the PI with rigid biphenyl side chain only, (b) the PI with flexible alkyl side chain only, (c) the PI containing both rigid benzene biphenyl side chain and flexible alkyl side chain.

4. Conclusions

We have synthesised a novel functional diamine (N0) containing a TPA unit and biphenyl unit. Furthermore, a series of PAAs and PIs were synthesized from CBDA, TFDB, N0 and C12. All PI films showed high transmittance in the wavelength range of 400–700 nm. Besides, an effect of the side chain structure on pretilt angles of the LC cells fabricated with the PIs was investigated. PI2 containing both rigid biphenyl side chain and flexible alkyl side chain performed a better rubbing resistance than PI3 only containing flexible alkyl side chain. PI2 could align LCs vertically before and after rubbing treatment, but PI3 could induce LCs vertical alignment only before rubbing treatment, after rubbing process, PI3 aligns LCs parallel. PI1, only after rubbing process, could induce LCs parallel alignment. We can propose that introduction of rigid biphenyl side groups within the PI films used as vertical LCs alignment layer could improve rubbing resistance. Besides, all PIs could align LCs

View Article Online
DOI: 10.1039/C5RA08521G

uniformly. Furthermore, thermal stability of PIs was improved with the increase of the rigid biphenyl side chains. The PIs with a good rubbing resistance and other excellent performance, like PI3, could be used for advanced LCDs like vertically aligned LCDs.

Acknowledgements

This work was supported by National Natural Science Foundation of China (Grant no. 51173115), the Ministry of Education (the Foundation for Ph.D. training, Grant no. 20110181110030) of China.

References

1 D. J. Liaw, K. L. Wang, Y. C. Huang, K. R. Lee, J. Y. Lai and C. S. Ha, Prog. Polym. Sci., 2012, 37, 907.

2 X. Y. Chen, V. T. Hoang, D. Rodrigue and S. Kaliaguine, RSC Adv., 2013, 3, 24266.

3 X. Y. Chen, V. T. Hoang, D. Rodrigue and S. Kaliaguine, RSC Adv., 2014, 4, 12235.

4 H. Shima, M. M. Hossain and J. R. Hahn, RSC Adv., 2014, 4, 41204.

5 S. Ramakrishnan, M. Dhakshnamoorthy, E. J. Jelmy, R. Vasanthakumari and N. K. Kothurkar, RSC Adv., 2014, 4, 9743.

6 Y. Niu, X. Zhang, J. Zhao, Y. Tian, Y. Li and X. Yan, RSC Adv., 2014, 4, 28456.

7 H. J. Yen, C. L. Tsai, P. H. Wang, J. J. Lin and G. S. Liou, RSC Adv., 2013, 3, 17048.

8 S. l. Xia, Z. Sun, L. f. Yi and Y. H. Wang, RSC Adv., 2013, 3, 14661.

9 X. Wang, H. Wang, L. Luo, J. Huang, J. Gao and X. Liu, RSC Adv., 2012, 2, 9463.

10 H. Hatoh, M. Ishikawa, J. Hirata, Y. Hisatake and T. Yamamoto, Appl. Phys. Lett., 1992, 60, 1806.

11 K. H. Yang, Jpn. J. Appl. Phys., 1992, 31, L1603

12 R. Kiefer, B. Weber, F. Windscheid and G. Baur, In: Proceedings of the 12th International Display Research Conference, Hiroshima, 1992.

13 M. Oh-e, M. Ohta, S. Aratani and K. Kondo, In: Proceedings of the 15th International Display Research Conference, Hamamatsu, 1995.

View Article Online
DOI: 10.1039/C5RA08521G

14 H. Seiberle and M. Schadt, In: Proceedings of the 18th International Display Research Conference, Seoul, 1998.

15 A. Takeda, S. Kataoka, T. Sasaki, H. Chida, H. Tsuda, K. Ohmuro, T. Sasabayashi, Y. Koike and K. Okamoto, SID Symposium Digest of Technical Papers, 1998, 29, 1077.

16 K. H. Kim, K. Lee, S. B. Park, J. K. Song, S. N. Kim, and J. H. Souk, In: Proceedings of the 18th International Display Research Conference, Seoul, 1998.

17 S. S. Kim, SID Symposium Digest of Technical Papers, 2005, 36, 1842.

18 J. Ma, Y. C. Yang, Z. G. Zheng, J. Shi, W. Cao, Displays, 2009, 30, 185.

19 A. Lien, R. A. John, M. Angelopoulos, K. W. Lee, H. Takano, K. Tajima and A. Takenaka, Appl. Phys. Lett., 1995, 67, 3108.

20 T. Sakai, K. Ishikawa and H. Takezoe, Liq. Cryst., 2002, 29, 47.

21 Z. Liu, F. Yu, Q. Zhang, Y. Zeng and Y. Wang, Eur. Polym. J., 2008, 44, 2718.

22 M. liu, Z. Sun and Y. H. Wang, Chinese Journal of Liquid Crystals and Displays, 2013, 28, 19.

23 Y. Shao, Y. F. Li, X. Zhao, X. L. Wang, T. Ma and F. C. Yang, J. Polym. Sci., 2006, 44, 6836.

24 I. S. Chung and S. Y. Kim, Macromolecules, 2000, 33, 3190.

25 S. B. Lee, G. J. Shin, J. H. Chi, W. C. Zin, J. C. Jung , S. G. Hahm, M. Ree and T. Chang, Polymer, 2006, 47, 6606.

26 S. I. Kim, M. Ree, T. J. Shin and J. C. Jung, J. Polym. Sci., 1999, 37, 2909.

27 Y. J. Lee, J. G. Choi, I. Song, J. M. Oh and M. H. Yi, Polymer, 2006, 47, 1555.

28 B. Chae, S. B. Kim, S. W. Lee, S. I. Kim, W. Choi, B. Lee, M. Ree, K. H. Lee and J. C. Jung, Macromolecules, 2002, 35, 10119.

29 X. Wang, P. Zhang, Y. Chen, L. Luo, Y. Pang and X. Liu, Macromolecules, 2011, 44, 9731.